

Figure 5 Avalanche threshold. The initial angle is $\varphi = 32^\circ$; the height of the minimum perturbation triggering an avalanche is plotted as a function of the additional tilt $\delta\varphi$. We use an inclined tube to release from a very small height additional glass beads practically one by one at one spot on the surface⁸. As soon as an avalanche has occurred, the delivery is stopped and the added mass m is measured. We calculate an equivalent added height $H = [(3/\pi)[\tan^2(\beta)]m/\rho]^{1/3}$ as the beads form a cone of slope $\beta \approx 30^\circ$ and mean density $\rho = 1.48 \text{ g cm}^{-3}$ on top of the existing layer. This height decreases roughly linearly with $\delta\varphi$, as indicated by the short-dashed line. The error bars are the statistical error over ten measurements.

different in nature from those for upward propagation.

Careful observation of the motions of grains shows that these reach their limiting velocity very rapidly and go straight down the slope. The lateral spread of the triangular avalanches can thus be interpreted as due to the friction exerted by the rolling grains on their lateral neighbours being sufficient to set some of them into motion. On the other hand, in upward propagation, the grains start to roll down spontaneously because the grains located below them are already gone. The threshold of this uphill motion is compatible with the condition that the thickness difference between the initial layer and the new static layer is larger than a typical height, taken as one particle diameter for the short-dashed line in Fig. 1.

We observed the same two types of behaviour with other materials (crushed walnut shells and Sinai sand). We can thus think of comparing these avalanches with other types of avalanche (of snow or rocks) occurring in a geological context. In these cases, the triggering, amplification and velocity of the avalanches are of practical importance. Comparisons can already be made with some snow avalanches, where triangular tracks are observed at their origin⁵. In our experiment we have observed triangular avalanches exclusively in the case where a thin layer is located over a surface creating a strong friction. In all the other cases, the avalanche front propagates uphill. This suggests that the variation of friction coefficient across the layer also plays an important role in snow avalanches. □

Received 30 November 1998; accepted 11 March 1999.

1. Reynolds, O. On the dilatancy of media composed of rigid particles in contact. *Phil. Mag.* **20**, 469–481 (1885).
2. Bagnolds, R. A. The shearing and dilatation of dry sand and the 'singing' mechanism. *Proc. R. Soc. Lond. A* **295**, 219–232 (1966).
3. Rajchenbach, J. in *Physics of Dry Granular Media* (eds Hermann H., Hovi, J.-P. & Luding, S.) 421–440 (Kluwer, Dordrecht, 1998).
4. Caponieri, M., Douady, S., Fauve, S. & Laroche, C. in *Mobile Particulate Systems* (eds Guazzelli, E. & Oger, L.) 331–366 (Kluwer, Dordrecht, 1995).
5. McClung, D. *Avalanche Handbook* (Mountaineers, Seattle, 1993).
6. Pouliquen, O. & Renault, N. Onset of granular flows on an inclined rough surface: dilatancy effects. *J. Phys. II France* **6**, 923–935 (1996).
7. Pouliquen, O. Scaling laws in granular flows down rough inclined planes. *Phys. Fluids* (in the press).
8. Held, G. A. et al. Experimental study of critical-mass fluctuations in an evolving sandpile. *Phys. Rev. Lett.* **65**, 1120–1123 (1990).

Acknowledgements. This work was supported by the University Paris VII through BQR97.

Correspondence and requests for materials should be addressed to A.D. (e-mail: daerr@physique.ens.fr).

Desorption–ionization mass spectrometry on porous silicon

Jing Wei*, Jillian M. Buriak† & Gary Siuzdak*

*Departments of Molecular Biology and Chemistry, The Scripps Research Institute, BCC157, 10550 North Torrey Pines Road, La Jolla, California 92037, USA

†Department of Chemistry, Purdue University, West Lafayette, Indiana 47907-1393, USA

Desorption mass spectrometry has undergone significant improvements since the original experiments were performed more than 90 years ago¹. The most dramatic change occurred in the early 1980s with the introduction of an organic matrix^{2–4} to transfer energy to the analyte. This reduces ion fragmentation but also introduces background ions from the matrix. Here we describe a matrix-free strategy for biomolecular mass spectrometry based on pulsed-laser desorption–ionization from a porous silicon⁵ surface. Our method uses porous silicon to trap analytes deposited on the surface, and laser irradiation to vaporize and ionize them. We show that the method works at femtomole and attomole levels of analyte, and induces little or no fragmentation, in contrast to what is typically observed with other such approaches^{6–11}. The ability to perform these measurements without a matrix^{3,4,12,13} also makes it more amenable to small-molecule analysis. Chemical¹⁴ and structural¹⁵ modification of the porous silicon has enabled optimization of the ionization characteristics of the surface. Our technique offers good sensitivity as well as compatibility with silicon-based microfluidics and microchip technologies.

The broad success of matrix-assisted desorption/ionization is related to the ability of the matrix to incorporate and transfer energy to the analyte^{3,4,12,16}. For instance, in matrix-assisted laser desorption/ionization (MALDI)⁴, the analyte is typically dissolved into a solid ultraviolet-absorbing organic acid matrix which vaporizes upon pulsed-laser radiation, carrying with it the analyte¹⁶. Direct desorption/ionization without matrix has been extensively studied on a variety of surfaces^{6–11} but has not been widely used because of the rapid molecular degradation that is usually observed upon direct exposure to laser radiation. However, just as secondary ion mass spectrometry (SIMS) has had a profound effect on surface science¹⁷, the utility of direct laser desorption/ionization for biomolecular analysis could be highly beneficial owing to dramatically simplified sample preparation, elimination of matrix background ions, and other advantages we describe here.

Our matrix-free desorption approach uses the porous silicon surface to trap the analyte molecules and, because of its high absorptivity in the ultraviolet¹⁸, act as an energy receptacle for the laser radiation. The experimental protocol for desorption/ionization on silicon (DIOS) (see Methods and Fig. 1) involves the generation of porous silicon from flat crystalline silicon by using a simple galvanostatic etching procedure¹⁵. A micrometres-thick porous layer with a nanocrystalline architecture is produced that exhibits bright photoluminescence upon exposure to ultraviolet light^{5,19}. The thickness, morphology, porosity, resistivity and other characteristics of the material are readily modulated through the choice of silicon-wafer precursor and etching conditions (see Methods). Freshly etched porous silicon surfaces are hydrophobic owing to the metastable, silicon-hydride termination, but through Lewis-acid-mediated¹⁴ or light-promoted hydrosilylation reactions²⁰, the surface can be easily stabilized and functionalized as required. Because of the high stability of the hydrophobic, hydrosilylated surfaces to aqueous media, these surfaces can be reused repeatedly (see Methods) with little degradation^{14,20}. Photopatterning of the

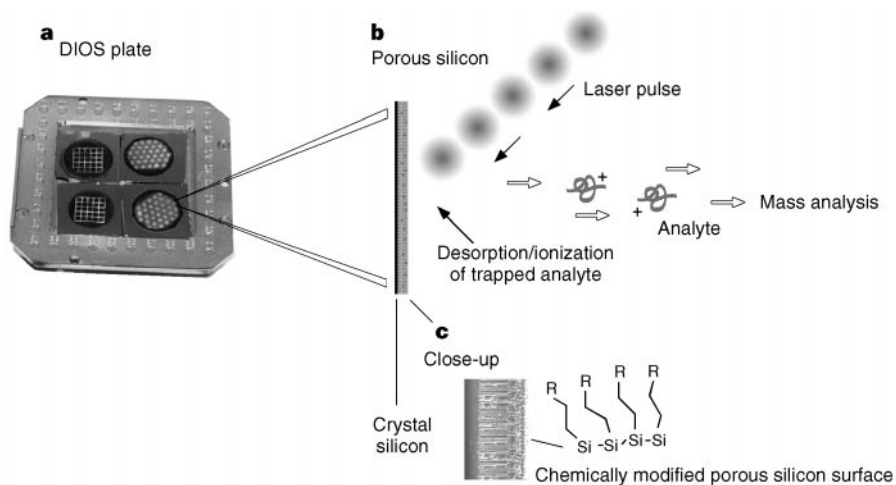


Figure 1 Experimental configuration for the DIOS-MS experiments. **a**, Four porous silicon plates are placed on a MALDI plate. Each of the porous silicon plates contains photopatterned spots or grids prepared through illumination of n-type silicon with a 300-W tungsten filament through a mask and an $f/50$ reducing lens. **b**, The silicon-based laser desorption/ionization process, in which

the sample is placed on the porous silicon plate and allowed to dry, followed by laser-induced desorption/ionization mass spectrometry. **c**, Cross-section of porous silicon, and the surface functionalities after hydrosilylation; R represents phenyl or alkyl chains.

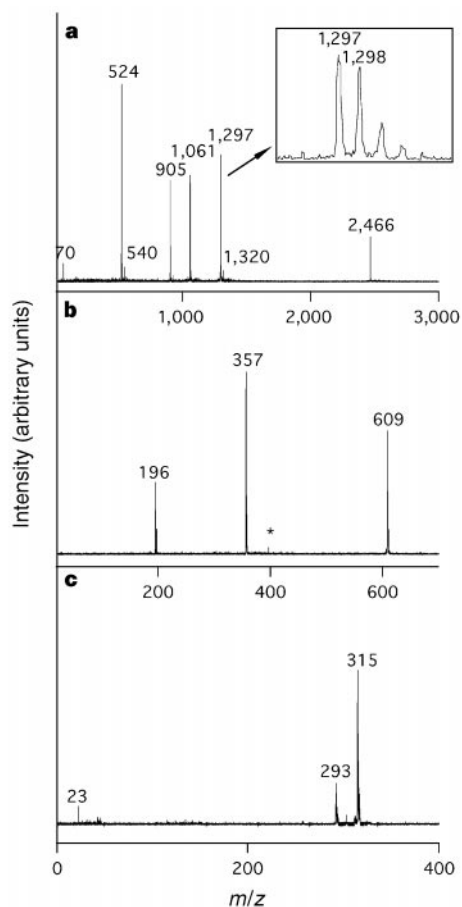


Figure 2 Examples of mass spectral data obtained with DIOS. **a**, The DIOS mass spectrum of a mixture of five peptides (2 pmol each), including a four-residue peptide (MRFA in single-letter amino-acid code) at m/z 524, des-arg-bradykinin (m/z 905), bradykinin (m/z 1,061), angiotensin (m/z 1,297), and adrenocorticotrophic hormone (m/z 2,466). The small peaks at m/z 540 and m/z 1,320 are oxidized MRFA and a sodium adduct of angiotensin, respectively. The signal of m/z 70 corresponds to a surface background ion (possibility $C_5H_7^+$). Insert, spectrum

showing the isotopes of angiotensin and that the resolution is not affected by the porous silicon surface. **b**, The DIOS mass spectrum of a mixture of three small molecules, including caffeine (m/z 196), an antiviral drug WIN (m/z 357) and reserpine (m/z 609) (1 pmol each). A small signal (asterisk) was an impurity from caffeine. **c**, The DIOS mass spectrum of 10 pmol *N*-octyl β -D-glucopyranoside (m/z 293) and its sodium adduct ion (m/z 315). The sodium ion (m/z 23) itself was also detected.

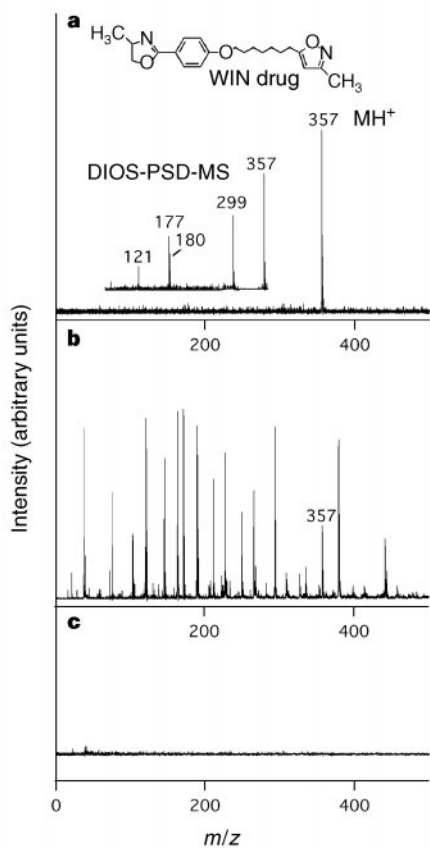


Figure 3 Analysis of WIN antiviral drug (500 fmol) using different desorption/ionization techniques. **a**, DIOS-MS spectrum of WIN. Accurate mass measurements were obtained on WIN with a time-of-flight reflectron instrument, typically to within 10 p.p.m. (the limit of accuracy of this instrument in this mass range). The inset spectrum represents post-source decay fragmentation measurements on WIN. These results are consistent with results from electrospray ionization tandem mass spectrometry experiments. **b**, MALDI-MS of same amount of antiviral drug using α -cyano-4-hydroxycinnamic matrix. **c**, No signal was obtained from any of the compounds tested using laser desorption mass spectrometry off the gold MALDI plate.

surfaces is possible and has been used galvanostatically to etch 5×5 -well plates in a 1.1-cm^2 area on n-type silicon, allowing for the analysis of 25 samples in series²¹ (Fig. 1). We used surface photopatterning to identify where on the uniform porous silicon surface the sample had been placed.

The porous silicon surfaces were tested with a broad range of compounds. Examples of DIOS mass spectrometry (DIOS-MS) on peptides, caffeine, an antiviral drug molecule (WIN), reserpine and *N*-octyl β -D-glucopyranoside are shown in Fig. 2. Over thirty other compounds ranging in size from 150 to 12,000 daltons, including carbohydrates, peptides, glycolipids, natural products and small drug molecules, were tested and their molecular ion was observed with little or no fragmentation. Although MALDI-MS analysis is also possible for small molecules²² and matrix suppression can be achieved under certain circumstances²³, matrix interference presents a real limitation (Fig. 3) that a matrix-less technique such as DIOS does not encounter.

DIOS has some unique features that make it useful for a variety of biomolecules. Peptides generate a good signal from the deposition of 700 attomol of material (also the limit of detection in our MALDI instrument on this compound) and allow the analyte to be analysed even in a saturated salt solution. For example, spectra from the peptide des-arg-bradykinin (Fig. 4) were easily obtained from

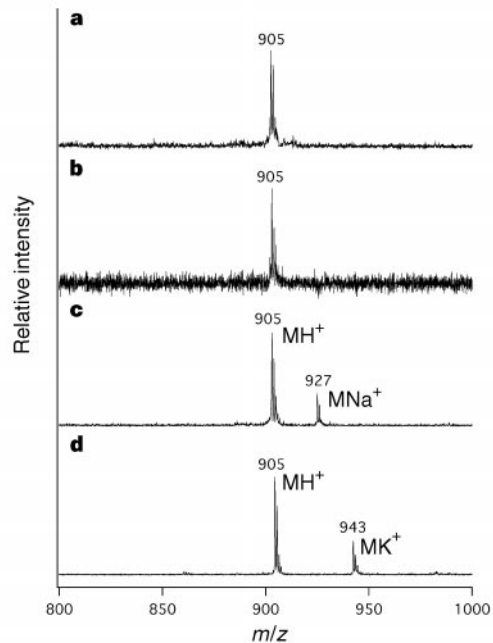


Figure 4 DIOS mass spectra of des-arg-bradykinin using small quantities of sample and in the presence of salt. **a-d**, DIOS mass spectra with: **a**, 7 fmol; **b**, 700 attmol; **c**, 2 pmol in the presence of a 2 M NaCl; and **d**, 2 pmol in a saturated solution of K_3PO_4 buffer solution. All spectra shown were generated from an n-type mesoporous silicon surface modified with an ethyl phenyl termination; they are the average of 128 shots with a nitrogen laser (337 nm) at an intensity, typical of MALDI experiments, of 2 to $50 \mu\text{J}$ per pulse.

saturated K_3PO_4 , 2.0 M NaCl, and 2.0 M Tris solutions, although higher laser intensities were required for these analyses. No silicon-containing adducts were ever detected in DIOS-MS spectra which might interfere with these analyses, indicating the inert nature of the porous silicon material. In addition, the resolution obtained in the analysis of compounds (Fig. 2) from DIOS was identical to that in MALDI analyses, as were post-source decay fragmentation measurements made on peptides and small molecules (Fig. 3). However, the DIOS post-source decay small-molecule measurements would ordinarily be impossible to perform with a MALDI reflectron instrument because of matrix interference.

The observation of a variety of intact ions directly emanating from these surfaces suggests that porous silicon has properties such as high surface area²⁴ and strong ultraviolet absorption¹⁸ that may enhance pulsed laser desorption and ionization. The porous structure on the surface is essential for desorption and ionization, because control experiments done with glass, with air-oxidized single-crystal silicon of (100) orientation, with 0.25-mm-thick, 60 Å-pore silica-gel thin-layer chromatography plates, or with gold MALDI plates (Fig. 3) gave no significant ion signal. A variety of etching conditions²⁵ were used to produce microporous (≤ 2 nm pore sizes) and mesoporous (2–50 nm pore sizes) silicon²⁴. Both n-type mesoporous samples and p-type micro- or mesoporous samples were effective in generating signals, but the surfaces with smaller pore sizes typically gave a more intense ion signal. To understand the ionization mechanism better, we used the DIOS approach on four porous silicon surfaces, each containing different surface modifications, including hydrogen (native), dodecyl, ethyl phenyl ($-\text{CH}_2\text{CH}_2\text{C}_6\text{H}_5$), and oxide. Of the porous silicon surfaces tested, most could effectively generate ions. However, the more hydrophobic surfaces, and in particular an ethylphenyl-terminated surface, typically gave better signals for the same quantity of analyte from an aqueous medium¹⁴. Dissolving the sample in methanol/ H_2O at a 1:1 v/v ratio also provided a stronger signal, indicating that

analyte penetration into the porous silicon is important. The energy for analyte release from the surface may be transferred from silicon to the trapped analyte through vibrational pathways or as a result of the rapid heating of porous silicon producing H₂ (ref. 26) that releases the analyte. Alternatively, as porous silicon absorbs hydrocarbons from air or while under vacuum^{27,28}, rapid heating/vaporization of trapped hydrocarbon contaminants or solvent molecules may augment the vaporization and ionization of the analyte embedded in the porous silicon. The observation of DIOS-MS background ions (*m/z* < 100) at high laser intensities, consistent with aliphatic hydrocarbons, indicates that they may play a role in desorption/ionization.

The potential application of DIOS-MS is broad. The surface activity could be changed through derivatization with receptors²⁹, aiding the identification of ligands. In addition, the enhanced signal obtained from the ethyl phenyl surface suggests that significant improvements can be made to DIOS-MS through further investigation of surface modifications. Most existing MALDI mass spectrometers could be used to perform DIOS simply by making modifications to the MALDI sample plate (Fig. 1). Moreover, porous silicon material is inexpensive and its production simple. Porous silicon can be readily integrated with existing silicon-based technology¹⁵, allowing, for example, its application into miniaturized chip, microfluidic chemical reactors that are lithographically etched into crystalline silicon wafers. For instance, porous silicon features as small as 20 μm and 100 nm can be produced through standard optical techniques²¹ and ion implantation³⁰, respectively. In short, as a new desorption/ionization approach, DIOS-MS offers sensitivity, high tolerance to contaminants, no matrix interference and, because the surface properties of porous silicon can easily be tailored, more control over biomolecular mass spectrometry. □

Methods

Effective porous silicon samples for DIOS could be prepared from either n- or p-type silicon according to these general procedures. For n-type: P-doped, (100) orientation, 0.65 Ω cm resistivity Si wafers were etched for 1–3 min using +71 mA cm⁻² current density with illumination by a 300-W tungsten filament bulb in a 1:1 solution of ethanol/49% HF (aq). For p-type: B-doped, (100) orientation, 0.01 Ω cm resistivity Si wafers were etched at 37 mA cm⁻² current density in the dark for 3 h in a 1:1 solution of ethanol/49% HF (aq).

DIOS, MALDI and laser desorption (off a gold surface) experiments were performed on a Voyager DE-STR, time-of-flight mass spectrometer (PerSeptive Biosystems) using a pulsed nitrogen laser (Laser Science) operated at 337 nm. Once formed, ions were accelerated into the time-of-flight mass analyser with a voltage of 20 kV. Porous silicon surfaces for DIOS analysis were mounted onto the MALDI probe by adhesive tape. Analytes were dissolved in a deionized H₂O or H₂O/methanol mixture at concentrations typically ranging from 0.001 to 10.0 μM. Aliquots (0.5–1.0 μl; corresponding to 0.5 femtomol to 100 picomol analyte) of solution were deposited onto the porous surfaces and allowed to dry before DIOS mass-spectrometry analysis. After multiple usage, the porous silicon surface-regeneration procedure necessitated rinsing surfaces with deionized H₂O and methanol sequentially, and finally immersing the surface overnight in a 1:2 v/v methanol/H₂O mixture. Surfaces were rinsed with deionized H₂O then with methanol and allowed to dry before applying the analyte.

Received 17 November 1998; accepted 1 March 1999.

1. Thomson, J. J. Rays of positive electricity. *Phil. Mag.* **20**, 752–767 (1910).
2. Liu, L. K., Busch, K. L. & Cooks, R. G. Matrix-assisted secondary ion mass spectra of biological compounds. *Anal. Chem.* **53**, 109–113 (1981).
3. Barber, M., Bordoli, R. S., Sedgwick, R. D. & Tyler, A. N. Fast-atom bombardment of solids as an ion source in mass spectrometry. *Nature* **293**, 270–275 (1981).
4. Karas, M. & Hillenkamp, F. Laser desorption ionization of proteins with molecular mass exceeding 10,000 daltons. *Anal. Chem.* **60**, 2299–2301 (1988).
5. Canham, L. T. Silicon quantum wire array fabrication by electrochemical and chemical dissolution of wafers. *Appl. Phys. Lett.* **57**, 1046–1048 (1990).
6. Zenobi, R. Laser-assisted mass spectrometry. *Chimia* **51**, 801–803 (1997).
7. Zhan, Q., Wright, S. J. & Zenobi, R. Laser desorption substrate effects. *J. Am. Soc. Mass Spectr.* **8**, 525–531 (1997).
8. Hrubowchak, D. M., Ervin, M. H., Wood, M. C. & Winograd, N. Detection of biomolecules on surfaces using ion-beam-induced desorption and multiphoton resonance ionization. *Anal. Chem.* **63**, 1947–1953 (1991).

9. Varakin, V. N., Lunchev, V. A. & Simonov, A. P. Ultraviolet-laser chemistry of adsorbed dimethylcadmium molecules. *High En. Chem.* **28**, 406–411 (1994).
10. Wang, S. L., Ledingham, K. W. D., Jia, W. J. & Singhal, R. P. Studies of silicon nitride (Si₃N₄) using laser ablation mass spectrometry. *Appl. Surf. Sci.* **93**, 205–210 (1996).
11. Posthumus, M. A., Kistemaker, P. G., Meuzelaar, H. L. C. & Ten Noever de Brauw, M. C. Laser desorption–mass spectrometry of polar nonvolatile bio-organic molecules. *Anal. Chem.* **50**, 985–991 (1978).
12. Macfarlane, R. D. & Torgerson, D. F. Californium-252 plasma desorption mass spectroscopy. *Science* **191**, 920–925 (1976).
13. Siuzdak, G. in *Mass Spectrometry for Biotechnology* 162 (Academic, San Diego, 1996).
14. Buriak, J. M. & Allen, M. J. Lewis acid mediated functionalization of porous silicon with substituted alkenes and alkynes. *J. Am. Chem. Soc.* **120**, 1339–1340 (1998).
15. Cullis, A. G., Canham, L. T. & Calcott, P. D. J. The structural and luminescence properties of porous silicon. *J. Appl. Phys.* **82**, 909–965 (1997).
16. Hillenkamp, F., Karas, M., Beavis, R. C. & Chait, B. T. Matrix-assisted laser desorption ionization mass spectrometry of biopolymers. *Anal. Chem.* **63**, A1193–A1202 (1991).
17. Benninghoven, A., Rüdenauer, F. G. & Werner, H. W. (eds) *Secondary Ion Mass Spectrometry* 1227 (Wiley, New York, 1987).
18. Amato, G. & Rosenbauer, M. in *Optoelectronic Properties of Semiconductors and Superlattices* (eds Amato, G., Delerue, C. & Bardeleben, H.-J.v.) 3–52 (Gordon and Breach, Amsterdam, 1997).
19. Sailor, M. J. & Lee, E. J. Surface chemistry of luminescent silicon nanocrystallites. *Adv. Mater.* **9**, 783–793 (1997).
20. Stewart, M. P. & Buriak, J. M. Photopatterned hydrosilylation on porous silicon. *Angew. Chem. Int. Edn* **37**, 3257–3261 (1998).
21. Doan, V. V. & Sailor, M. J. Photolithographic fabrication of micron-dimension porous Si structures exhibiting visible luminescence. *Appl. Phys. Lett.* **60**, 619–620 (1992).
22. Lidgard, R. & Duncan, M. W. Utility of matrix-assisted laser desorption ionization time-of-flight mass spectrometry for the analysis of low molecular weight compounds. *Rapid Commun. Mass Spectr.* **9**, 128–132 (1995).
23. Knochenmuss, R., Dubois, F., Dale, M. J. & Zenobi, R. The matrix suppression effect and ionization mechanisms in matrix-assisted laser desorption/ionization. *Rapid Commun. Mass Spectr.* **10**, 871–877 (1996).
24. Canham, L. T. in *Properties of Porous Silicon* (ed. Canham, L. T.) 83–88 (Institution of Electrical Engineers, London, 1997).
25. Hérimo, R. in *Properties of Porous Silicon* (ed. Canham, L. T.) 89–96 (Institution of Electrical Engineers, London, 1997).
26. Ogata, Y. H., Kato, F., Tsuboi, T. & Sakka, T. J. Changes in the environment of hydrogen in porous silicon with thermal annealing. *Electrochem. Soc.* **145**, 2439–2444 (1998).
27. Canham, L. T. in *Properties of Porous Silicon* (ed. Canham, L. T.) 154–157 (Institution of Electrical Engineers, London, 1997).
28. Canham, L. T. in *Properties of Porous Silicon* (ed. Canham, L. T.) 44–50 (Institution of Electrical Engineers, London, 1997).
29. O'Donnell, M. J., Tang, K., Koster, H. & Smith, C. L. High density, covalent attachment of DNA to silicon wafers for analysis by MALDI-TOF mass spectrometry. *Anal. Chem.* **69**, 2438–2443 (1997).
30. Schmuki, P., Erickson, L. E. & Lockwood, D. J. Light emitting micropatterns of porous Si created at surface defects. *Phys. Rev. Lett.* **80**, 4060–4063 (1998).

Acknowledgements. We thank J. Boydston, Z. Shen, R. G. Cooks and M. Duncan for their comments, T. Hollenbeck for suggesting the acronym DIOS, K. Harris for his initial analyses of porous silicon surfaces, and M. P. Stewart and T. Geders for preparing oxidized and p-type porous silicon samples. G.S. is grateful for partial funding by an NIH grant; J.M.B. thanks Purdue University for support and the Camille and Henry Dreyfus Foundation for a New Faculty Award.

Correspondence and requests for materials should be addressed to J.M.B. and G.S. (e-mail: buriak@purdue.edu and siuzdak@scripps.edu).

Growing range of correlated motion in a polymer melt on cooling towards the glass transition

Christoph Bennemann*‡, Claudio Donati*†, Jörg Baschnagel‡ & Sharon C. Glotzer*

* Center for Theoretical and Computational Materials Science, and Polymers Division, National Institute of Standards and Technology, Gaithersburg, Maryland 20899, USA

† Dipartimento di Fisica e Istituto Nazionale per la Fisica della Materia, Università di Roma 'La Sapienza', Piazzale Aldo Moro 2, I-00185 Roma, Italy
‡ Institut für Physik, Johannes Gutenberg Universität, Staudinger Weg 7, 55099 Mainz, Germany

Many liquids cooled to low temperatures form glasses (amorphous solids) instead of crystals. As the glass transition is approached, molecules become localized and relaxation times increase by many orders of magnitude¹. Many features of this 'slowing down' are reasonably well described² by the mode-coupling theory of supercooled liquids³. The ideal form of this theory predicts a dynamical critical temperature T_c at which the